Preprints of the 18th IFAC World Congress
Milano (Italy) August 28 - September 2, 2011

Tokamak Plasma Shape and Current H_∞ Controller Design in Multivariable Cascade System

Yuri V. Mitrishkin*. Alexei V. Kadurin, Alexander Y. Korostelev*****

** V.A. Trapezinikov Institute of Control Sciences of the Russian Academy of Sciences, 117997 Moscow, Russia, Profsoyuznaya Street, 65 (phone: +7 910 424 6556, fax: +7 499 234 6426, e-mail: y_mitrishkin@hotmail.com)*
*** V.A. Trapezinikov Institute of Control Sciences of the Russian Academy of Sciences, 117997 Moscow, Russia, Profsoyuznaya Street, 65 (e-mail: nirudak@mail.ru)*
**** Bauman Moscow State Technical University, 105005 Moscow, Russia (email: akorostel@gmail.com)*

Abstract: The paper is devoted to the design and simulation of a multivariable cascade system with a H_∞ controller in the outer loop which has the goal to track plasma shape and current in a tokamak by manipulation of control current references. These currents flow in magnetic coils located around a tokamak vacuum vessel and generate a poloidal magnetic field to confine the high-temperature plasma inside the vessel. For the controller *K* design a mixed-sensitivity objective was achieved by minimization of the H_∞-norm of the stacked and shaped transfer function *S/KS* where the sensitivity *S* is a matrix transfer function from a plant external disturbance to plasma shape and current signals. The H_∞ approach was applied in the outer cascade to the plant consisting of two inner loops of the system. The first scalar inner loop stabilizes a plasma unstable vertical position speed at about zero. The second inner multivariable loop was preliminary designed to decouple control currents. The cascade system was simulated with plasma-physics DINA code in the divertor phase of the plasma current ramp-up stage for two scenarios: the ITER 15 MA scenario and another one with a new set of scenario control currents given by the control system from the initial simulation. The motivation of the H_∞ outer loop design is to enhance the robust stability margin of the system in comparison with the known system consisting of the series connection of the pseudo-inverse matrix and diagonal PII-controller with a double integrator in the outer multivariable loop without losing tracking accuracy. The H_∞ cascade control system showed about five times larger the robust stability margin estimated by means of singular values of the complementary sensitivity *T* in frequency domain.

1. INTRODUCTION

Tokamaks (Artsimovich, 1972, Wesson, 1997, Pironti and Walker, 2005) are the most perspective devices for producing energy from nuclear fusion. The confinement of high-temperature plasma in magnetic field at a sufficiently high pressure is the basic idea of the future thermonuclear reactor to get self-sustained thermonuclear reaction. The tokamak is a toroidal vacuum vessel with magnetic coils that is a magnetic confinement device with toroidal geometry. The tokamak works as follows. The gas (for instance a deuterium-tritium mixture) is pumped inside the vessel and is broken down by an induced electric field due to the external magnetic field change. So the gas is ionized, becomes the plasma which is able to interact with externally generated magnetic fields. Plasma is confined in the vessel by combined toroidal and poloidal magnetic fields. The toroidal magnetic field is generated by the electric current flowing in the toroidal coil. Poloidal fields are generated by the currents in poloidal coils surrounding the vessel (Fig. 1) and the plasma current is induced by a transformer action because the plasma is a conductor. Poloidal coils act as the primary of the transformer while the plasma acts as the secondary. Thus the magnetic fields produce an external magnetic pressure that balances the gas-kinetic pressure of the hot plasma.

Tokamak plasma position, shape, and current are controlled by magnetic fields of the poloidal coil currents. These currents are created by appropriate voltages that are applied to the coils. The main goal of the plasma magnetic control system is to track plasma scenario shape and current with bounded deviations on plasma current ramp-up stage and stabilize these parameters on the plasma current flat-top phase. We develop the plasma magnetic control system for ITER (International Thermonuclear Experimental Reactor, under construction in France).

There is a set of approaches of plasma position, shape and current control (see for instance Ariola and Pironti, 2008). The paper presents the design of an H_∞ plasma magnetic control system based on the cascade channel decoupling methodology developed in (Mitrishkin *et al.*, 2009). The prototype cascade system uses combination of diagonal PII-controller with pseudo-inverse matrix as plasma current and shape controller in the outer loop. In order to improve robust performance and robust stability and to achieve the desired

trade-off of those characteristics this controller has been replaced in the design by the multivariable H_∞ controller in the outer loop of the cascade structure.

Section 2 provides short description of the plasma nonlinear and linear models used for controller design and simulation. The robust plasma control problem is stated in section 3. The control system structure with the inner decoupling loop is described in section 4. The design of the plasma shape and current H_∞ controller is represented in section 5. Simulation results of cascade control systems with H_∞ and PII controllers on nonlinear plasma-physics DINA code are shown in section 6. Section 7 summarizes the results obtained.

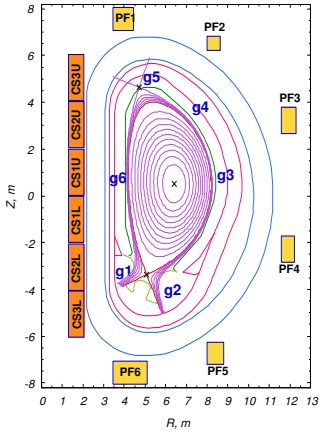

Fig. 1. ITER vertical cross-section. Location of the CS and PF coils, their numbering and six controlled gaps between separatrix and the first wall/divertor

2. PLANT MODEL UNDER CONTROL

2.1 Nonlinear Model

The tokamak plasma differential equation in the state space is a nonlinear electromagnetic Kirchhoff equation which describes the coupled magnetic system of conductors with currents including the plasma current (Dokuka *et al.,* 2007)

$$\frac{d}{dt}\Psi\left(I, I_p, \xi\right) + RI = Nu, \quad N = \begin{bmatrix} \Xi_{m\times m} \\ 0_{(n-m)\times m} \end{bmatrix} \tag{1}$$

where Ψ denotes the poloidal fluxes vector-function, I is the vector of currents in active and passive structures with n states, I_p is the total plasma current, R is the matrix of resistances, $\Xi_{m\times m}$ is the unit matrix corresponding to the voltage vector u on active coils, $\dim u = m$, $n > m$, $\xi = \left[\beta_p \quad l_i\right]^T$, β_p is the scalar proportional to the plasma pressure, l_i is the internal plasma inductance. Plasma equilibrium in the magnetic field is described by Grad-Shafranov equation (Wesson, 1997) which is connected with equation (1) and gives the nonlinear plant model to be controlled. Plasma current evolution is taken in accordance with the following condition $\bar{\Psi} = \int_{S_p} j\Psi dS_p / I_p = const$ where $\bar{\Psi}$ is the averaged poloidal flux over the plasma cross-section, j is the plasma current density, S_p is the plasma cross-section square. The nonlinear plasma model described above is implemented in DINA code (Khayrutdinov and Lukash, 1993, Lukash *et al.,* 2004).

2.2 Linear Model

After application of a linearization procedure (Ariola and Pitonti, 2008, Mitrishkin *et al.*, 2005) to nonlinear plasma equations one can obtain a plant linear equation around an equilibrium point of a plasma discharge scenario:

$$\dot{x} = Ax + Bu + E\delta\dot{\xi}, \quad y = Cx + F\delta\xi \tag{2}$$

where x is the state vector of passive and active currents deviations, $\dim x = n$, u is the vector of voltage variations on active coils, y is the output vector of plasma current variation, deviations of plasma geometric parameters, and variations of currents in active coils. For vertically elongated plasmas the vertical position is unstable resulting in a positive eigenvalue of matrix A in (2). Reduced linear models were used for the H_∞ controller design. Such models were created by truncation of modes corresponding to lower Hankel singular values in balanced realizations of (2) (Skogestad and Postlethwaite, 2005).

3. PLASMA CONTROL PROBLEM STATEMENT

Fig. 1 illustrates the ITER plasma vertical cross-section on a divertor stage (Plasma Performance Assessment, 2009). Plasma shape and current are defined by currents in central solenoid (CS) and poloidal fields (PF) coils. The diagnostic system is used to measure plant outputs: gaps between plasma boundary (separatrix) and the first wall/divertor at six points (g1…g6), the vertical position of the plasma magnetic axis, control currents in active coils as well as the total plasma current. The eddy currents in passive structures are not measured but may be estimated and used in a control law if necessary. Plant inputs are voltages on all CS and PF coils. The voltages are generated by power supplies which play the role of plant actuators and are controlled multiphase thyristor rectifiers (AC/DC convertors).

The control system should provide: (i) tracking of the discharge scenario parameters (g1..g6) and the plasma current with specified accuracy, (ii) rejection of external disturbances of a minor disruption type represented as drops of β_p and l_i in plasma models, (iii) plasma control on the long time interval of scenario including the plasma current ramp-up stage and quasistationary tokamak operation mode. The latter requirement is closely connected to robust stability of control system, as long as the plant under control is nonlinear and changes its properties in time, that is the plant is different at different scenario points. However, it was discovered that variation of plasma properties over significant time intervals of the scenario is not so large (Mitrishkin *et al.*, 2011). Thus, it is possible to achieve plasma control goals during the part of the divertor phase on the plasma current ramp-up stage by using a linear controller based on a linearized model for one of scenario points. On the limiter phase of the plasma ramp-up stage with a transition to the divertor phase one can switch

the controller to another one without change of its structure to keep the closed-loop stability and proper performance.

4. DECOUPLING INNER LOOP IN THE CASCADE SYSTEM STRUCTURE

In the ITER documentation (Plasma Performance Assessment, 2009) the plasma magnetic control scheme contains two basic loops: a scalar loop for plasma vertical speed control and a multivariable loop for gaps, plasma current and CS/PF currents control. In (Mitrishkin *et al*., 2009, Mitrishkin *et al*., 2011) the cascade control system for ITER was suggested and developed. In that proposal the inner cascade is used for CS/PF currents control and the references of this cascade are the outputs of the plasma shape and current controller. Such engineering solution makes possible to decouple channels of tracking the scenario currents and essentially simplify the adjustment of these channels in practice in comparison with a controller designed for the whole set of plant outputs. Consequently the general cascade structure of the plasma magnetic control system for ITER consists of three loops: fast loop for vertical speed suppression which is separated from the relatively slow loops for the CS/PF currents control as well as the plasma shape and current control (Fig. 2).

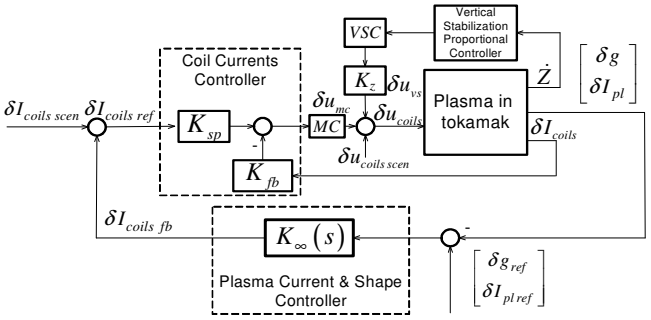

Fig. 2. Control system structural schematic. VSC is the vertical stabilization converter; MC is the main converter consisting of 11 power supplies; the unit $K_z = [0\ 0\ 0\ 0\ 0\ 0\ -1\ -1\ 1\ 1\ 0]^{\mathrm{T}}$ represents the connection of the VSC to the PF2-PF5 coils

To design the inner control loop the square *sub-plant* was considered in which the inputs number is equal to outputs number. Here 11 outputs are current variations in CS/PF coils and 11 voltages on these coils are manipulated input variables. Active coils, passive structures, and plasma filament in a tokamak are strongly magnetically coupled so the easiest way to control CS and PF currents independently is to decouple them in the square plant mentioned above. At this design stage the linearized plasma model was used. All inputs and outputs of the model are deviations from their equilibrium values at the scenario point about which the model is linearized. The linear coupled sub-plant model is represented in the state space form as follows:

$$\dot{x} = A_1 x + B_1 u,\ y = C_1 x \tag{3}$$

where $x \in \mathbb{R}^{127}$ is the state vector specifically variations of currents in active and passive structures, $u \in \mathbb{R}^{11}$ is the control voltages variations vector (inputs) and $y \in \mathbb{R}^{11}$ is the vector of measured CS/PF currents variations (outputs). The decoupled control law is $u = K_{sp} r - K_{fb} y$ where r is the vector of reference CS/PF currents. If one substitutes this control law into (3) we obtain the closed-loop equation

$$\dot{x} = \left(A_1 - B_1 K_{fb} C_1\right) x + B_1 K_{sp} r\ . \tag{4}$$

Let us denote $\Lambda = A_1 - B_1 K_{fb} C_1$ in (4) and then the decoupling problem is formulated as follows: find matrix K_{fb} so that the matrix Λ becomes a *diagonal* matrix with equal diagonal elements and find the matrix K_{sp} to meet the condition: $y = r$ at a zero frequency. It can be shown that the matrix transfer function of the closed-loop system (4) will be diagonal at all frequencies and will contain identical first-order units on its diagonal. To achieve that, we perform the reduction of the linear model (3) to 11 states, which gives square matrices A_2, B_2, and C_2 of the 11×11 size. After that we can specify a desired matrix Λ which will give the required feedback K_{fb} and the set-point K_{sp} matrices

$$K_{fb} = B_2^{-1}\left(A_2 - \Lambda\right) C_2^{-1},\ K_{sp} = -B_2^{-1} \Lambda C_2^{-1}\ . \tag{5}$$

Thus the *closed* inner control loop with *reduced* sub-model and matrices K_{fb}, K_{sp} given in (5) will have identity matrix gain Ξ at zero frequency when $\dot{x} = 0$ in (4): $y_0 = C_2 x_0 = C_2\left[-\Lambda^{-1} B_2 K_{sp} r_0\right] = \Xi\, r_0$. Due to the reduced linearized model used in the synthesis, the proposed control law $u = K_{sp} r - K_{fb} y$ applied to the original model (3) will give only approximate decoupling. However simulations show that a sufficient accuracy of the decoupling is achieved. All diagonal elements of matrix Λ are chosen to be equal to –1.0, and the multivariable inner closed loop system becomes decoupled into 11 independent first order loops with the same time constant of 1.0 s.

5. H_∞ OUTER LOOP DESIGN IN CASCADE STRUCTURE

The design objective is to incorporate the multivariable H_∞ controller *K* into the outer loop of the cascade structure for plasma shape and current control. The problem of the H_∞ controller synthesis is formulated as mixed-sensitivity design (Skogestad and Postlewaith, 2005)

$$J\left[K(s)\right] = \left\| \begin{matrix} W_1(s)\, S(s) \\ W_2(s)\, K(s)\, S(s) \end{matrix} \right\|_\infty \underset{K(s)}{\rightarrow} \min\ . \tag{6}$$

The optimization criterion *J* in (6) is the H_∞-norm of the block matrix consisting of sensitivity $S = (I + GK)^{-1}$ and *KS* where the sensitivity *S* is a matrix transfer function from the plant external disturbance to gap displacements and current signals. The criterion *J* is minimized over the class of

stabilizing matrix controllers $K(s)$ for the linear plant model $G(s)$. The optimization problem (6) is solved in separate frequency ranges which are determined in (6) by the scalar weighting functions $w_1(s)$ and $w_2(s)$, placed on the diagonals of matrix transfer functions W_1 and W_2 respectively. The solution of the optimization problem (6) gives the trade-off between robust stability and robust performance of the outer loop of the cascade control system.

The characteristic frequency of the slow inner loop was specified in section 4 as 1 s^{-1}. This value was selected as ω_B^* parameter for a weighting function

$$w_1(s) = \left(m^{-1/2}s + \omega_B^*\right)^2 / \left(s + \omega_B^* a^{1/2}\right)^2. \qquad (7)$$

The scalars m and a in (7) were adjusted to get the best performance in the simulations on nonlinear DINA code. In (7) the second order transfer function was used because it provided faster system response in comparison with the first order case. The weight w_2 was chosen as a constant: $w_2 = 1$.

After the weighting functions were found the H_∞ controller was designed and simulated on the linear plasma model in MATLAB environment for a preliminary estimate of the controller performance. The best controllers were selected from the resulting set of synthesized controllers taking into account performance and frequency responses. The H_∞ design procedure includes scaling of multivariable plant (Skogestad and Postlethwaite, 2005) thus adjustment of weighting functions parameters is simplified and the acceptable balance of the output signals (gaps and plasma current) is achieved. In Fig. 3 one can see maximum and minimum singular values plots of sensitivity S and complementary sensitivity $T = GK(I + GK)^{-1}$ of the closed-loop system with H_∞ and with PII-controllers specifically

$$\sigma_i(S) = +\sqrt{\lambda_i\left(SS^H\right)}, \sigma_i(T) = +\sqrt{\lambda_i\left(TT^H\right)}, S^H = S^T(\bar{s})$$

where $i = 1,\ldots,7$. The parameters of the weighting function $w_1(s)$ in (7) used for controller design are as follows: $m = 1.5,\ a = 0.0001,\ \omega_B^* = 1$. The controller was synthesized for the linear model at the point I_p = 8.5 MA of the ITER scenario 2 with the nominal plasma current I_p=15 MA. Maximums of the maximal singular values of S and T obtained are significantly smaller for the system with the H_∞ controller (Fig. 3) specifically

$$\|S_{PII}\|_\infty / \|S_{H_\infty}\|_\infty = 6.1597 / 1.2550 = 4.9081,$$
$$\|T_{PII}\|_\infty / \|T_{H_\infty}\|_\infty = 5.9921 / 1.2054 = 4.9711,$$
$$\|S\|_\infty = \sup_\omega \bar{\sigma}\left[G(j\omega)\right], \bar{\sigma} = \max \sigma_i.$$

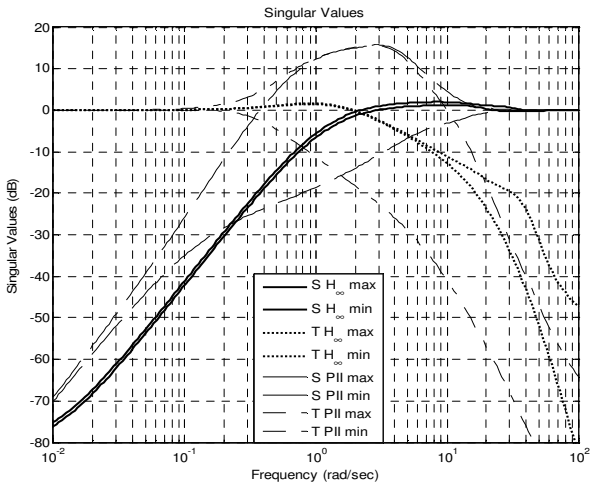

Fig. 3. Maximum and minimum singular values of S (solid, dash) and T (dot, dash-dot) of closed-loop system with H_∞ and PII controllers respectively.

The H_∞ norms of S and T are connected with the 2-norms of the input/output signals and stability margin in presence of the plant model multiplicative output uncertainty Δ by the following relations (Skogestad and Postlewaith, 2005):

$$\|y\|_2 \le \|S\|_\infty \|d\|_2,\ \|\Delta\|_\infty \le 1/\|T\|_\infty.$$

Thus the system with the H_∞ controller provides more effective external disturbances rejection and robust stability factor of about 5 times better than the system with the PII-controller.

6. CONTROL SYSTEM SIMULATION ON DINA CODE

6.1 Simulation with the Given Scenario

The numerical simulation of the cascade control system with the channel decoupling in the inner loop and the H_∞ controller in the outer loop for plasma shape and current control was done using the nonlinear plasma model realized by DINA code on the interval of the ITER scenario from the point I_p = 8.5 MA to the point I_p = 15 MA and further comprising the start of the plasma current flat-top phase. This period corresponds to the time interval from 35 s to 105 s of the ITER scenario and includes the part of plasma current ramp-up stage from X-point formation up to the start of quasi-stationary stage. Fig. 4 shows plots of gap values over the whole simulation interval of the system with the H_∞-controller comparing to the simulation of the PII-controller at the same conditions. Fig. 5 presents plots of the plasma current for both systems and its deviation from the scenario reference respectively.

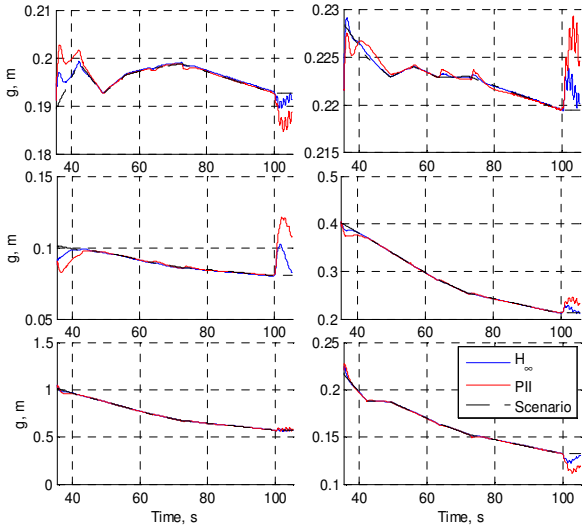

Fig. 4. Values of 6 gaps versus time: blue corresponds to the H_∞ -controller and red belongs to the PII-controller

The plots of deviations of CS/PF currents from their scenario values taken from the ITER database for the H_∞ system are given in Fig. 6. It can be seen that coil currents significantly differ from scenario reference currents. Relative values of errors listed in Table 1 show that such large deviations from scenario are too large. This mismatch is probably related to the fact that the ITER scenario was computed on a different code with different physics assumptions and other adjustments, and as a result plasma equilibrium configurations for each scenario point were caused by different values of coil currents.

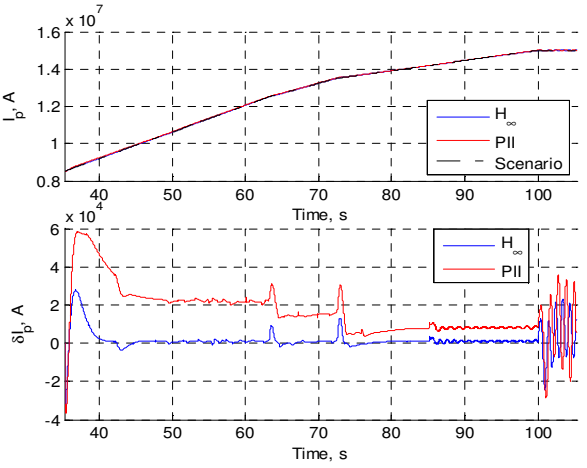

Fig, 5. Absolute value and deviation of plasma current

The control performance indexes in Table 1 were calculated relative to output vectors tracking error $\Delta x(t) = x(t) - x_{ref}(t)$

$$\varepsilon_x(t) = \left\|\Delta x(t)\right\|_2 / \left\|x_{ref}(t)\right\|_2, \text{avg}\,\varepsilon_x = \sqrt{\int_{T_1}^{T_2} \left\|\Delta x\right\|_2^2 dt \Big/ \int_{T_1}^{T_2} \left\|x_{ref}\right\|_2^2 dt}$$

where $x(t)$ is the simulated value of the corresponding vector, $x_{ref}(t)$ is the scenario value of this vector, $\|\bullet\|_2$ is the 2-norm in the Euclidean space of the corresponding dimension, $\varepsilon_x(t)$ is the tracking error, and $\text{avg}\,\varepsilon_x$ is the average relative error over time interval $[T_1, T_2]$.

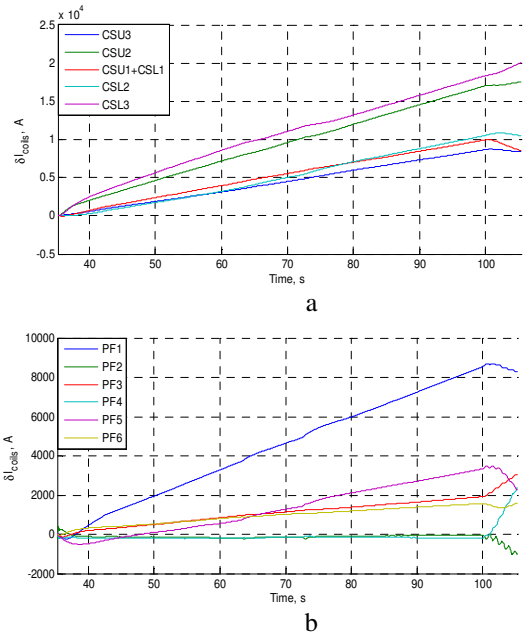

Fig. 6. CS (a) and PF (b) current deviations

Table 1. Comparison of the simulation results

Errors %	PII standard scenario	H_∞ standard scenario	PII modified scenario	H_∞ modified scenario
$max\ \varepsilon_g$	5.2	4.5	3.07	2.73
$avg\ \varepsilon_g$	1.4	0.78	0.72	0.31
$max\ \varepsilon_{Ip}$	1.1	0.4	0.81	0.53
$avg\ \varepsilon_{Ip}$	0.18	0.046	0.16	0.13
$max\ \varepsilon_I$	34.8	36.8	1.8	2.86
$avg\ \varepsilon_I$	26.14	24.7	0.75	0.99
$max\ \varepsilon_{ICS}$	57.3	67.3	3.18	5.13
$avg\ \varepsilon_{ICS}$	41.4	52.3	1.56	1.60
$max\ \varepsilon_{IPF}$	21.8	12.9	0.75	2.07
$avg\ \varepsilon_{IPF}$	13.2	8.15	0.46	0.74

6.2 Simulation with the Modified Scenario

The coil currents obtained from the results of the simulation performed were used as modified scenario coil currents in a new simulation, that is the scenario was modified. Another controller was used for this new simulation which was synthesized with the same parameters of the weighting function $w_1(s)$ in (7) but a linear model at a new point was taken as a plant model. This point is located approximately in the middle of the simulation period opposed to the point in its beginning as in the previous case. It was supposed that this could improve control performance on the whole interval of divertor phase at the plasma current ramp-up stage, and

especially on its final part that is the quasi-stationary stage. Simulation results are presented in Fig. 7, 8.

6.3 Comparison of Simulation Results

In Fig. 7, 8 one can see that the new simulations with modified scenario coil currents result in significantly lower coil currents deviations while preserving good tracking of gaps and plasma current. Table 1 gives relative deviations of the output signals from their scenario values for the systems with PII- and H_∞-controllers and for simulations with standard scenario coil currents and modified ones.

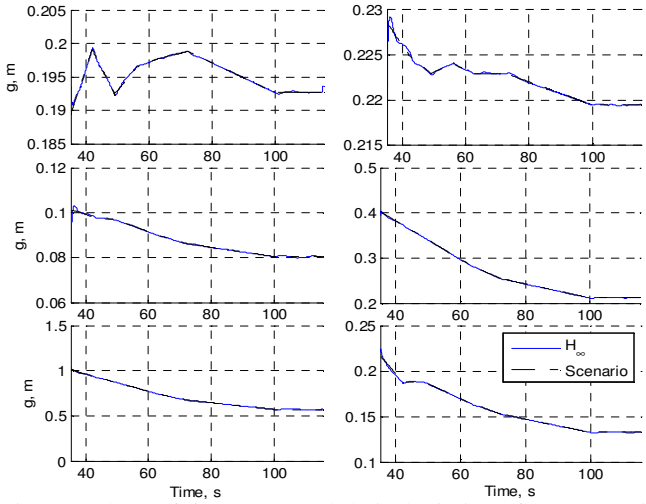

Fig. 7. Values of 6 gaps (a) and their deviations from scenario (b) in simulation with modified scenario CS/PF coil currents

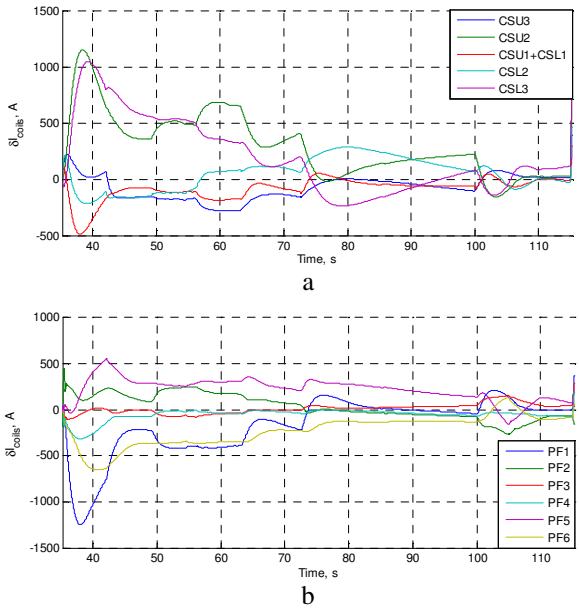

Fig. 8. CS (a) and PF (b) currents deviations in simulations with modified CS/PF coil currents

7. CONCLUSIONS

The paper presents the design and simulation of the control system for tokamak plasma position, shape and current based on the combination of the channel cascade decoupling approach and H_∞ optimization to advance the system robustness. The system gives the accurate ITER modified scenario tracking on plasma current ramp-up phase from the X-point formation up to flat-top stage on nonlinear DINA code. This was achieved by essentially improving the trade-off between plasma shape/current and CS/PF currents during the control process. The H_∞ cascade control system showed larger robust stability margin than the system with the PII controller in the outer loop specifically about five times larger.

REFERENCES

Ariola, M. and A. Pironti (2008) *Magnetic Control of Tokakmak Plasmas.* Springer-Verlag London Limmited.

Artsimovich, L.A. (1972). Tokamak Devices, *Nuclear Fusion*, Vol. 12, pp. 215-252.

Dokuka, V.N., A.V. Kadurin, Y.V. Mitrishkin, and R.R. Khayrutdinov (2007). Synthesis and Modeling of H_∞ Plasma Magnetic Control System in Tokamak-reactor. *Automatica i Telemechanica,* No 8, p. 126-145 (in Russian).

Khayrutdinov, R.R. and V.E. Lukash (1993). Studies of Plasma Equilibrium and Transport in a Tokamak Fusion Device with the Inverse-Variable Technique. *Journal Comp. Physics*, Vol. 109, pp. 193-201.

Lukash, V.E., V.N. Dokuka, and R.R. Khayrutdinov (2004). Software-computing DINA Complex in MATLAB System for Solving Plasma Control Problems in Tokamaks. *Issues of atomic science and technology. Series: Nuclear Fusion,* Vol. 1, pp. 40-49 (in Russian).

Mitrishkin, Y.V., V.N. Dokuka, and R.R. Khayrutdinov (2005). Linearization of ITER Plasma Equilibrium Model on DINA Code. *Proc. of the 32nd EPS Conference on Plasma Physics*, *Tarragona, Spain*, ID P5.080.

Mitrishkin, Y.V., A.Y. Korostelev, V.N. Dokuka, and R.R. Khayrutdinov (2009). Design and Modeling of ITER Plasma Magnetic Control System in Plasma Current Ramp-Up Phase on DINA Code. *Proc. of the 48th IEEE Conference on Decision and Control*, *Shanghai, P.R. China*, pp. 1354-1359.

Mitrishkin, Y.V., A.Y. Korostelyov, V.N. Dokuka, and R.R. Khayrutdinov (2011). Design and Modeling of Two-level Magnetic Plasma Control System of Tokamak-reactor. *Plasma Physics*, Vol. 37, No 4, pp. 307-349 (in Russian).

Pironti, A. and M. Walker (2005). Fusion, Tokamaks, and Plasma Control. *IEEE Control Systems,* Vol. 25. No 5, pp. 30-43.

Plasma Performance Assessment (2009). ITER_D_22HGQ7 v 3.0.

Skogestad, S. and I. Postlethwaite (2005). *Multivariable Feedback Control* (2nd ed.). John Wiley & Sons Ltd.

Wesson, J. (1997). *Tokamaks* (2nd ed.). Clarendon Press, Oxford.